

**Enhanced heat transfer for isoperibolic semibatch reactors:
a kinetic free sizing criterion.**

Francesco Maestri, Ester Rossi, Renato Rota*

Politecnico di Milano, Dip. di Chimica, Materiali e Ingegneria Chimica “G. Natta”,
Piazza Leonardo da Vinci, 32 – 20133 Milano – Italy

*renato.rota@polimi.it, fax: +39 0223993180

Abstract

Whenever the productivity of an indirectly cooled, isoperibolic semibatch reactor (SBR) must be enhanced keeping the reaction temperature nearly constant, an additional heat transfer surface with respect to that provided by the reactor jacket only must be installed. In these cases, internal coils are normally adopted, which additional surface is however intrinsically limited and not fully available since from the beginning of the supply period. However, a suitable fraction of the overall heat transfer surface can be installed on an external reactor recycle loop: this allows also for a simpler monitoring of the reaction system by comparing the measured temperature to a nearly constant target value. In this work a kinetic-free sizing criterion has been developed for isoperibolic SBRs (both homogeneous and heterogeneous), through which the required external heat transfer surface can be easily estimated.

Keywords:

Semibatch Reactor (SBR); Isoperibolic Conditions; Heat Transfer; Safety; Reactor Monitoring.

1. Introduction

Relatively fast and exothermic reactions of the fine chemical and pharmaceutical industry are normally performed in indirectly cooled semibatch reactors^{1,2}, where the conversion rate and the related heat evolution can be spread over a sufficiently wide time period, according with the heat transfer characteristics of the involved equipment³⁻⁹.

However, when an intrinsically fast reaction process is significantly exothermic (as occurs for the sake of example with several nitration, ethoxylation and hydrogenation reactions¹⁰), the heat removal rate through the reactor jacket or half tube only can be insufficient to guarantee a satisfactory reactor productivity, since it would call for too long dosing periods in order to control the reaction heat evolution¹¹.

In these cases, starting the coreactant dosing at a lower coolant (and hence initial) temperature than the average desired one, would increase the heat removal rate because of a higher difference between internal and coolant temperatures. However, adopting a lower initial temperature, the system reactivity is also depressed, which could even lead to a dangerous accumulation of the desired coreactant and to the final thermal loss of control of the reaction².

Instead, the installation of an enhanced heat transfer surface, allows for significantly increasing the heat removal rate from the system and hence for reducing the cycle time on the reactor without affecting the initial system reactivity.

The heat transfer surface increase is normally obtained through internal coils¹¹. However, the surface enhancement is in this case limited because of geometric constraints related to the reactor geometry. Moreover, the presence of internal coils lowers the free space within the reaction vessel and hence the productivity per batch.

In any case, the contribution provided by internal surfaces (that is, by the reactor jacket or half tube, as well as by internal coils) is not fully available since from the beginning of the supply period, but it becomes progressively available as the reactor is filled by the coreactant dosing.

The progressive increase of the available heat transfer surface leads to a normal decrease of the reaction temperature under isoperibolic conditions, even if the system reactivity does not undergo any significant drop up to the end of the supply period^{4,8}.

If such a temperature drop is excessive (which is typical of systems characterized by low values of the Westerterp number), the reaction course might be unregular because of too variable conditions with respect to what the chemical recipe states, with detrimental consequences, among the others, on the final product quality^{12,13}.

In these cases, isothermal operating conditions could be adopted, controlling the reactor temperature through the coolant flowrate and inlet temperature¹⁴.

However, such a control logic is more complicated to be implemented than simple isoperibolic conditions in which the reactor temperature is allowed to vary within a sufficiently narrow range.

Whenever the reaction system is not characterized by significant changes of its physical properties, all the aforementioned goals can be matched allocating a suitable fraction of the overall heat transfer surface on a reactor recycle loop, that is, realizing a parallel cooling circuit through a properly sized external heat exchanger (see Figure 1). Such an equipment is much less subjected to size limitations than an internal coil and, being the related surface fully available since from the beginning, it can significantly mitigate the reaction temperature variations during the supply period: this ensures a much better control of the reaction even under simple isoperibolic conditions.

This is a welcome feature for both safety and product quality reasons, when unwanted impurities can be partially formed outside a recommended temperature range^{12,13}.

Moreover, the adoption of an external exchanger can yield a significant increase not only of the installed surface, but also of the overall heat transfer efficiency: in fact, if the reaction mass can be easily pumped in all the phases of the process, a plate heat exchanger¹⁵ on the reactor recycle line could be installed rather than a standard shell and tube one, achieving heat transfer coefficients one order of magnitude higher than those provided by a shell and tube exchanger as well as by a well

stirred vessel¹⁵⁻¹⁷. This allows for a significantly lower exchanger size at a given heat transfer efficiency.

The smoothing effect on the reactor temperature time profile during the coreactant dosing has also a potential advantage in terms of reactor monitoring¹⁸⁻²⁰.

Under standard isoperibolic conditions, in fact, the target temperature time profile is not in general suitable for checking the expected system reactivity during the dosing period, due to its decreasing behavior^{4,8}.

In these cases (as well as when dealing with reaction systems undergoing a significant variation of their physical properties) the general energy criterion developed by Maestri and Rota can be used for monitoring the SBR operation without any limitation¹⁹. Such a criterion is in fact based on a set of energy KPIs, which can be easily on-going calculated through fully available process variables.

However, if through an enhanced external surface the target temperature variation is effectively minimized, even the reactor temperature can be directly used as a process variable to check the expected reactivity level of the reaction system by simply comparing the actual reactor temperature with a nearly constant target value.

It should be stressed that the energy criterion¹⁹ remains in any case the most general approach, since it is not affected by any change of the system physical properties and is based on the on-going monitoring of energy parameters characterized by a universal target value. The target temperature value is instead peculiar of any reaction system^{4,8}. However, whenever possible, a reactor monitoring based on the reaction temperature only is undoubtedly more straightforward^{14,21}.

It must be finally noticed that even if the only adoption of an external heat transfer surface would provide a theoretically constant temperature for the most part of the supply period, a standard heat transfer surface is in any case already available on any equipment and is useful to avoid a needless oversizing of the external surface²¹. Moreover, a separate cooling system could be adopted for the jacket and the external exchanger: such a redundancy strategy is in particular welcome when dealing

with dangerous runaway reactions for which a cooling system failure is a critical scenario²²⁻²⁵, which expected frequency of occurrence must be therefore minimized.

In this work, for both homogeneous and heterogeneous isoperibolic SBRs, a general and simple sizing criterion is provided, through which, for a given allowable temperature variation during the dosing period, the required external heat transfer surface can be easily estimated.

The use of the criterion has been finally presented taking into exam a potential runaway process of the agrochemical industry (that is, the mixed acid nitration of 4-chloro benzotrifluoride), which is industrially performed in enhanced heat transfer reactors, because of safety and productivity constraints^{26,27}.

2. Mathematical model

In order to develop a design criterion to size with a minimum calculation effort the external heat transfer surface for making the operation of an isoperibolic SBR quasi-isothermal, the mathematical model of the reactor must be formerly written in a suitable dimensionless form.

The model equations for an isoperibolic SBR in which an exothermic reaction $\nu_A A + \nu_B B \rightarrow \nu_C C + \nu_D D$ occurs (either in a homogeneous or in a heterogeneous system) has been extensively discussed in the process safety literature^{3-9,28}.

However, in all the cited references, the heat transfer surface for removing the reaction heat within the reactor energy balance is an increasing function of time: this because of the progressive wetting of the internal surface (either jacket or coil) as the reaction vessel is filled.

Naming A the dosed coreactant and B the reactant initially loaded in the reactor, the mass balance equation expressed in terms of B conversion, $\zeta = 1 - n_B/n_{B0}$, can be written as:

$$\frac{d\zeta}{dt} = \frac{\nu_B}{n_{B0}} r^{\text{eff}} V_r \quad (1)$$

Here t is the time, ν_B the stoichiometric coefficient of the initially loaded reactant, n_{B0} the number of moles of such a reactant initially loaded in the reactor, r^{eff} the effective conversion rate, and V_r the reaction volume (which changes in time due to the co-reactant dosing).

Equation (1) can be recast in the following dimensionless form:

$$\frac{d\zeta}{d\vartheta} = \nu_A \text{Da RE } f \text{ e}^{\left[\gamma_{\text{app}}\left(1-\frac{1}{\tau}\right)\right]} \quad (2)$$

where ν_A is the stoichiometric coefficient of the coreactant A, ϑ is the dimensionless time (defined assuming as a reference value the supply period), $\text{Da} = k_R \cdot t_{\text{dos}} \cdot C_{B0}^{n+m-1}$ is the Damköhler number, being k_R the kinetic constant evaluated at the reference temperature, T_R , t_{dos} the dosing time, C_{B0} the initial concentration of reactant B, while n and m are the order of reaction with respect to reactant A and B, respectively. $\gamma_{\text{app}} = E_{\text{app}}/(RT_R)$, is an apparent activation energy in dimensionless form (corresponding to the microkinetic activation energy for homogeneous systems as well as for heterogeneous systems operated in the slow reaction regime, and to its half for heterogeneous systems operated in the fast reaction regime²⁹), and τ is the dimensionless temperature. The expressions of the so-called reactivity enhancement factor (RE) and of the function f (which is the only factor containing the functional dependence of the conversion rate on ϑ and ζ) depend on both the reacting phase and the reaction regime⁸. In particular, for homogeneous reaction systems $\text{RE} = \left(\frac{\nu_B}{\nu_A}\right)^{1-n}$ and $f = \frac{(\vartheta-\zeta)^n(1-\zeta)^m}{(1+\varepsilon\vartheta)^{n+m-1}}$ where $\varepsilon = V_{\text{dos},l}/V_{r0}$ is the relative volume increase at the end of the supply period; for heterogeneous slow reaction systems $\text{RE} = \left(\frac{\nu_B}{\nu_A}\right)^{1-n} m_B^m$ (being m_B the distribution coefficient of B between the dispersed and continuous phases) and $f = \frac{(\vartheta-\zeta)^n(1-\zeta)^m}{(\varepsilon\vartheta)^{n-1}}$ when the reaction occurs in the dispersed phase, while $\text{RE} = \left(\frac{\nu_B}{\nu_A}\right)^{1-n} m_A^n$ (being m_A the distribution coefficient of A between the continuous and dispersed phases) and $f = \frac{(\vartheta-\zeta)^n(1-\zeta)^m}{(\varepsilon\vartheta)^n}$ when the reaction occurs in the continuous phase; for heterogeneous fast reaction systems $\text{RE} = \frac{6}{d_{b0}} m_B^{\frac{m+1}{2}} C_{B0}^{\frac{1-n-m}{2}} \left(\frac{\nu_B}{\nu_A}\right)^{1-\frac{n}{2}} \left[\frac{2D_{Ld,B}}{(m+1)k_{n,m,Rd}}\right]^{\frac{1}{2}}$ and $f = \frac{(\vartheta-\zeta)^{\frac{n}{2}}(1-\zeta)^{\frac{m+1}{2}}(\varepsilon\vartheta)^{1-\frac{n}{2}}}{1+2.5\varepsilon\vartheta/(1+\varepsilon\vartheta)}$ when the reaction occurs in the dispersed phase, while $\text{RE} =$

$\frac{6}{d_{b0}} m_A^{\frac{n+1}{2}} C_{B0}^{\frac{1-n-m}{2}} \left(\frac{v_B}{v_A}\right)^{1-\frac{n}{2}} \left[\frac{2D_{Lc,A}}{(n+1)k_{n,m,Rc}}\right]^{\frac{1}{2}}$ and $f = \frac{(9-\zeta)^{\frac{n+1}{2}} (1-\zeta)^{\frac{m}{2}} (\varepsilon\theta)^{\frac{1-n}{2}}}{1+2.5\varepsilon\theta/(1+\varepsilon\theta)}$ when the reaction occurs in the continuous phase.

When the reactor is equipped with both an internal heat transfer surface and an external heat exchanger, the energy balance equation must take into account for both an indirect heat removal contribution through internal surfaces (such as the reactor jacket, half tube or internal coil) and an indirect heat removal term through the external heat exchanger on the reactor recycle loop. The two contributions must be separately expressed, since in the former the heat transfer surface is an increasing function of time, whereas in the latter the heat transfer surface is constant all along the process. Therefore, the energy balance equation provides:

$$\left[(n\tilde{C}_P)_c + (n\tilde{C}_P)_d\right] \frac{dT}{dt} = (F\tilde{C}_P)_{dos} (T_{dos} - T) + V_r r^{eff} (-\Delta\tilde{H}) - [(UA)_{ext} + (UA)_{int}] (T - T_{cool}) \quad (3)$$

Defining $R_H = (\rho C_P)_{dos} / (\rho C_P)_0$ the ratio between the volumetric heat capacities of the dosing stream and the reacting mixture, $\Delta\tau_{ad,0} = \frac{(-\Delta\tilde{H}_r)n_{A1}}{(\hat{\rho}\tilde{C}_P V)_0 T_R}$ a dimensionless adiabatic temperature rise, and being α a

flag parameter equal to 1 or $1/R_H$ for heterogeneous (liquid-liquid) or homogeneous SBRs respectively, the dimensional energy balance (3) can be recast in the following dimensionless form:

$$(1 + \alpha R_H \varepsilon \theta) \frac{d\tau}{d\theta} = R_H \varepsilon (\tau_{dos} - \tau) + \Delta\tau_{ad,0} \frac{d\zeta}{d\theta} - \varepsilon [Wt_{ext} + Wt_{int} (1 + \varepsilon \theta)] (\tau - \tau_{cool}) \quad (4)$$

where $Wt_{int} = (UA)_{0,int} t_{dos} / \varepsilon (\rho C_P V)_0$ and $Wt_{ext} = (UA)_{ext} t_{dos} / \varepsilon (\rho C_P V)_0$ are the Westerterp numbers related to the internal and external heat transfer surface, respectively: it can be noticed that whereas the internal Westerterp number is calculated on the basis of its initial UA value, the external one is constant all along the supply period, being the external surface fully available at any time.

As represented in Figure 1, the internal and external cooling circuits are in parallel and independent one from each other. For this reason, even adopting during the coreactant dosing the same inlet coolant temperature for both the circuits (which is typically the case at the industrial scale since the same coolant reservoir is shared by a number of equipment), the outlet coolant temperatures from the

internal and external cooling circuits can be different. However, when the mass flowrate through both the circuits is relatively high to make the coolant temperature increase negligible (which defines theoretically isoperibolic conditions²), the outlet coolant temperatures of both the circuits tend to be close to the inlet coolant temperature.

Along the same line presented in the literature^{3-9,28}, a weighted average coolant temperature can be defined as:

$$T_{\text{cool,eff}} = \frac{(F\tilde{C}_P T)_{\text{dos}} + [(UA)_{\text{ext}} + (UA)_{\text{int}}] T_{\text{cool}}}{(F\tilde{C}_P)_{\text{dos}} + (UA)_{\text{ext}} + (UA)_{\text{int}}} \quad (5)$$

which allows for lumping in a single heat removal term the cooling contribution of the dosing stream and of the heat exchange surfaces in Equation (4), which can be recast as:

$$(1 + \alpha R_H \varepsilon \vartheta) \frac{d\tau}{d\vartheta} = \Delta\tau_{\text{ad},0} \frac{d\zeta}{d\vartheta} - \varepsilon [R_H + Wt_{\text{ext}} + Wt_{\text{int}}(1 + \varepsilon\vartheta)] (\tau - \tau_{\text{cool,eff}}) \quad (6)$$

Equations (2) and (6) are valid all along the dosing period, that is for $0 \leq \vartheta < 1$. Once the whole coreactant amount has been fed (that is, at $\vartheta \geq 1$), the same equations hold true in which, however, the $\varepsilon\vartheta$ and τ_{dos} terms are replaced with ε and τ , respectively.

The initial conditions for the numerical integration of Equations (2) and (6) are: $\zeta=0$ and $\tau=\tau_0$ at $\vartheta=0$. Operating the SBR at a sufficiently low coreactant feed rate to achieve a much lower time scale consumption of the coreactant itself by the chemical reaction and an equally instantaneous removal of the evolved reaction heat, a pseudo steady state assumption for both the unreacted coreactant amount in the reactor and the reaction temperature becomes physically realistic¹⁸: as discussed in details elsewhere⁴⁻⁸, under such conditions (usually referred to as Quick Onset, Fair Conversion, Smooth Temperature profile or QFS conditions), the $d\zeta/d\vartheta$ and $d\tau/d\vartheta$ terms in the energy balance can be set equal to one and zero, respectively⁴⁻⁸. The energy balance equation simplifies therefore to the well-known expression of the target temperature profile for isoperibolic SBRs (in this case equipped with both an internal time-increasing heat transfer surface and an external constant one):

$$\tau_{\text{ta}} = \tau_{\text{cool,eff}} + \frac{1.05 \Delta\tau_{\text{ad},0}}{\varepsilon [R_H + Wt_{\text{ext}} + Wt_{\text{int}}(1 + \varepsilon\vartheta)]} \quad (7)$$

which represents the theoretical temperature profile allowing QFS conditions to be attained (note that the 1.05 safety factor suggested in the literature has been also included⁴⁻⁸).

As can be noticed, the target temperature profile (5) is in general a decreasing function of time all along the dosing period, because of the time-increasing heat transfer contribution of the internal surfaces.

The same decreasing trend can be expected for the actual temperature profile, which, under QFS conditions, approaches the target one for the most part of the supply period.

However, the external allocation of a suitable fraction of the whole heat transfer surface acts to mitigate the temperature drop during the dosing period.

Such a variation can be quantified through the difference between the target temperature values at the beginning of the supply period (when the available internal surface is minimum) and at the end of the supply period (when also the internal surface is fully available):

$$\Delta\tau_{ta} = \tau_{ta,0} - \tau_{ta,1} = \frac{R_H\tau_{dos} + (Wt_{ext} + Wt_{int})\tau_{cool} + 1.05 \Delta\tau_{ad,0}/\varepsilon}{R_H + Wt_{ext} + Wt_{int}} + \frac{R_H\tau_{dos} + [Wt_{ext} + Wt_{int}(1+\varepsilon)]\tau_{cool} + 1.05 \Delta\tau_{ad,0}/\varepsilon}{R_H + Wt_{ext} + Wt_{int}(1+\varepsilon)} \quad (8)$$

If $\tau_{dos} = \tau_{cool} = \tau_0$ (that is, the feed stream, the cooling medium, and the pre-charged reactant are at the same temperature), Equation (8) can be recast as follows:

$$R_{\Delta T} = \frac{\Delta T_{ta}}{\Delta T_{ad,0}} \times 100 = \frac{105}{\varepsilon} \left[\frac{1}{R_H + Wt_{ext} + Wt_{int}} - \frac{1}{R_H + Wt_{ext} + Wt_{int}(1+\varepsilon)} \right] \quad (9)$$

where $R_{\Delta T}$ is referred to as the ΔT ratio, being the ratio of the two relevant temperature differences characterizing the temperature time profile of the reaction, that is, the target temperature variation during the dosing period and the adiabatic temperature rise.

It must be noticed that the assumption $\tau_{dos} = \tau_{cool} = \tau_0$ is conservative for the final estimation of the external heat transfer surface: when the dosing stream is fed at a lower temperature than that of the reaction mass it provides in fact an additional heat removal contribution at the beginning of the supply period.

3. External heat transfer surface sizing criterion

In order to avoid a needless oversizing of the external surface and to monitor the system reactivity by comparing the target temperature value and the actual temperature profiles, the external heat exchange surface area must be at the same time large enough to mitigate the target temperature variation below a threshold value and not too large to keep a measurable difference between current and initial reaction temperatures. Under nearly isothermal QFS conditions and assuming $\tau_0 = \tau_{\text{cool}} = \tau_{\text{dos}}$, such a difference can be estimated through equation (7) using an average value of the target temperature computed at $t_{\text{dos}}/2$ (that is, at $\vartheta = 0.5$) as:

$$\Delta T_{\text{meas}} = T_{\text{ta}}(\vartheta = 0.5) - T_0 = \frac{1.05 \Delta T_{\text{ad},0}}{\varepsilon[R_{\text{H}} + Wt_{\text{ext}} + Wt_{\text{int}}(1 + \varepsilon/2)]} \quad (10)$$

If a very large heat transfer surface were adopted (that is, $Wt_{\text{ext}} + Wt_{\text{int}} \rightarrow \infty$), the target temperature profile would become constant and equal to the initial reactor temperature, as can be recognized from Equation (10). In this case, the reactor operation would be almost isothermal with $\tau = \tau_0$ and a reaction inhibition scenario (possibly leading to a dangerous accumulation of the coreactant) could not be detected through a simple comparison between target and actual reaction temperatures.

On the basis of the expected accuracy of the industrially available measurement devices, ΔT_{meas} values not lower than 2°C could be accepted^{16,18,21}.

Moreover, monitoring the reactor operation through the comparison of a target and an actual temperature value, the good industrial practice suggests installing more than one temperature measurement device¹⁸: this is helpful not only for redundancy reasons related to the process safety but also for accuracy reasons of the measurement itself, since averaging the signals of different devices minimizes the measurement error.

The proposed criterion requires to estimate an external heat exchange surface area able to keep at the same time the minimum $R_{\Delta T}$ value computed through equation (9), and a ΔT_{meas} value computed through equation (10) larger than about 2°C. However, in order to make the described sizing criterion

of practical industrial interest, a simple and general representation of the results of such equations should be useful.

Equation (9) is a function of five dimensionless parameters, that is $R_{\Delta T}$, R_H , ε , $W_{t_{int}}$ and $W_{t_{ext}}$. The dependence on the heat capacity ratio, R_H , can be managed apart by considering three different cases, corresponding to homogenous systems, heterogeneous (liquid-liquid) systems with an aqueous continuous phase and heterogeneous (liquid-liquid) systems with an organic continuous phase. Since the SBR thermal behavior is poorly dependent on value of the heat capacity ratio^{3-9,28} (except than for relatively low Westerterp numbers) the three characteristic R_H values suggested in the literature¹¹ for the aforementioned classes of reactions can be considered, namely: $R_H=1$ for homogeneous systems, and R_H equal to 0.4 and 2.5 for heterogeneous (liquid-liquid) systems with aqueous or organic continuous phase, respectively.

The internal Westerterp number, $W_{t_{int}}$, can be estimated through the graphical correlations provided by Westerterp and Molga¹¹, where, on the basis of a one-hour dosing time, the Westerterp numbers for well mixed reaction vessels equipped with either jacket or jacket and coil are provided as a function of the vessel volume and for systems initially containing an aqueous or an organic phase. $W_{t_{int}}$ can be then simply calculated multiplying the value taken from such graphical correlation by the actual dosing period (expressed in hours).

The relative volume increase, ε , is specified by the chemical recipe and it does not depend on the reactor size.

Therefore, for each reaction class (to which a R_H value corresponds), a set of graphical correlations are provided in Figures 2 to 4, each of which refers to a given $R_{\Delta T}$ value and plots $W_{t_{ext}}$ vs. $W_{t_{int}}$ values for a suitable range of ε values as a curve parameter.

On the basis of a number of industrial examples²²⁻²⁴ as well as of the data reported in the mentioned literature¹¹, ε reasonably ranges between 0.05 and 0.6, corresponding to a relative volume increase of 5 and 60% with respect to the initial reactor load.

A realistic range of variation of $R_{\Delta T}$ has been instead identified considering that most of the potential runaway reactions of interest of the fine chemical and pharmaceutical industry are characterized by $\Delta T_{ad,0}$ values ranging from 100 to 200°C²² and that the expected measurement error of an industrial temperature measurement device falls between 0.1 and 1°C^{16,18,21}. Accordingly, practical $R_{\Delta T}$ values ranging from 0.05 to 1 can be expected. Dividing such a range in four intervals, the results of the criterion in question can be summarized through five plots (identified by $R_{\Delta T}=0.05, 0.1, 0.2, 0.5$ and 1) for each reaction class. For intermediate values of the involved parameters, an intermediate external Westerterp number can be an estimation of the external exchanger surface, which is in any case practically approximated to the upper standard size^{15,17}.

It can be noticed that at given R_H , $R_{\Delta T}$ and ε values, the $W_{t_{ext}}$ vs. $W_{t_{int}}$ curves can show a maximum. This is due to the lower dependence of τ_{ta} on ϑ with respect to the case of a standard SBR equipped with an internal surface only, resulting from the inequality:

$$W_{t_{ext}} + W_{t_{int}} \gg \varepsilon \vartheta W_{t_{int}} \quad (11)$$

Since $\varepsilon\vartheta < 1$ all along the supply period, the growing rate of the constant $W_{t_{int}}$ term is higher than that of the time-variable $\varepsilon\vartheta W_{t_{int}}$ term. Therefore, as $W_{t_{int}}$ increases, $W_{t_{ext}}$ must rise at a decreasing rate, that is with a negative second order derivative, which explains why the plotted curves can show a maximum.

It can be also noticed that at a given R_H and $R_{\Delta T}$ value, the required $W_{t_{ext}}$ is lower at the higher ε values. This is also logical, since as ε increases the cooling enthalpy contribution of the dosing stream increases as well and therefore the cooling load on the heat transfer surfaces is lower.

A straightforward use of the described sizing criterion for the plant engineer can therefore be summarized through the following procedure, represented in Figure 5:

- 1) on the basis of the chemical recipe and of the literature data for the involved species and mixtures, the thermodynamic and process parameters of the reaction system can be estimated,

- in order to calculate $\Delta T_{ad,0}$ and ϵ . It should be stressed that no kinetic characterization of the system is required, with a significant saving of time and money¹⁸⁻²⁰;
- 2) for the reactor geometry and heat transfer characteristics (related to the installation of a jacket only or of a jacket and a coil) and for the type of initial phase loaded in the reactor (that is, aqueous or organic), the internal Westerterp number, Wt_{int} , for the system is estimated through the graphical correlations reported in Westerterp and Molga¹¹ and the expected coreactant dosing time. It must be noticed on this point that the Westerterp number values reported by Westerterp and Molga¹¹ are related to well mixed reaction vessels, so that a preventive check on the industrial mixer design and operation is recommended, especially when dealing with heterogeneous liquid-liquid systems²⁹;
 - 3) the minimum $R_{\Delta T}$ value is initially selected (that is, $R_{\Delta T} = 0.05$). This means that, if for the current system $\Delta T_{ad,0}$ is lower than 200°C, the corresponding ΔT_{ta} value is lower than 0.1°C, so that the target temperature variation can be considered practically negligible;
 - 4) from the proper graphical correlation of Figures 2 to 4 (corresponding to the R_H value for the system, and to the selected $R_{\Delta T}$ value), the external Westerterp number, Wt_{ext} , is read off and the external heat transfer surface is calculated using the desired dosing time and the expected heat transfer coefficient for the adopted type of external exchanger (that is, shell and tube, or plate^{15,17,21});
 - 5) with the calculated parameters, two checks are performed: the first one on the ΔT_{meas} value in comparison with its lower limit (that is, 2°C), and the second one on the estimated exchanger size, which could be in some cases subjected to upper limitations because of availability, operating, or installation reasons¹;
 - 6) if the checks described above are positive, the upper standard exchanger size is selected, and the operating parameters of the whole plant are finally calculated (such as, a suitable recycle

rate and the related pipe/nozzles diameters according with a satisfactory heat transfer efficiency and well balanced pressure drops^{15,17,21});

- 7) if a too low ΔT_{meas} or an unrealistic exchanger size have been estimated, the calculation sequence is repeated starting from point 3) for a higher $R_{\Delta T}$, the practical upper limit being the $R_{\Delta T}$ value corresponding to the maximum allowable target temperature variation, ΔT_{ta} , based on the accuracy of the adopted temperature measurement devices.

Once the external heat transfer surface has been selected according with the presented criterion, the SBR operation can be monitored by on-going measuring the actual reactor temperature, that must lie for most of the supply period in a suitable band around the average target value (say, $\pm 0.5^\circ\text{C}$, which implies ΔT_{ta} values of the order of 1°C). Such a band takes into account for any disturbance arising from the measurement noise as well as from slight variations of the system properties with the reaction extent.

Once the target temperature variation has been stabilized within a sufficiently narrow band, the actual temperature-time profile should at the limit overlap with the target one under the desired QFS conditions: however, this holds true for the most part of the coreactant dosing, but not in the first fraction of the supply period (where the triggering of the system must still occur) as well as in the last fraction of it (where the system reactivity physiologically drops because of the full consumption of the initially loaded reactant). Therefore, the comparison between the actual and the target temperature profiles must be limited to a central interval of the supply period, defining it through its boundaries and a suitable external band of variation (for instance, $\pm 1^\circ\text{C}$) of the actual temperature across the average target value.

As occurring with the more general energy criterion¹⁸⁻²⁰, also in this case the monitoring of the QFS reactor operation is performed through the comparison of a process parameter with its target value. However, the energy criterion is based on a set of KPIs that are on-going calculated and compared

with a target value equal to 100¹⁸⁻²⁰, whereas the criterion presented in this work compares the reactor temperature with a target temperature value, which is not general but peculiar of any reaction system. It must be finally mentioned that the proposed criterion is applicable to reaction systems whose physical properties do not significantly change during the supply period, as widely diffused in the fine chemical and pharmaceutical industries. However, when the reaction system undergoes a not negligible variation of its heat transfer properties, the more general energy criterion¹⁹ can be adopted for the preventive early warning monitoring of the reaction system.

4. Case study: heat transfer surface sizing for a nitration reaction

The described criterion has been applied to a case-study involving a potential runaway nitration process of the agrochemical industry, that is, the mixed acids nitration of 4-chloro benzotrifluoride^{26,27} (in the following referred to as 4-Cl BTF).

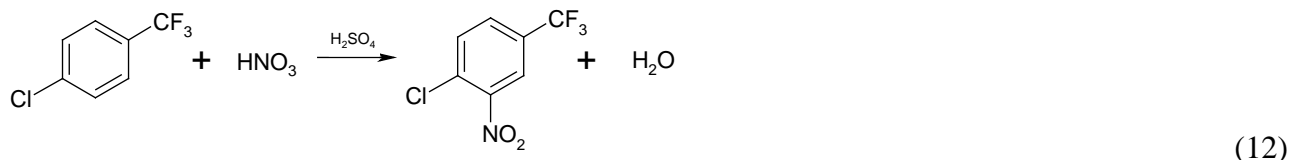
The reaction is assumed to be performed in indirectly cooled SBRs (internal diameter equal to about 1.3m and height equal to about 6m) equipped with a high turbulence stirring system to achieve an effective contact between the aqueous acidic phase (previously loaded in the reactor) and the organic phase (dosed in a suitable time period).

The height to diameter ratio of the reactor is relatively high, as occurs for a number of stirred vessels in which heterogenous reactions are performed²⁹ since it allows for a homogenous turbulence distribution within the reaction mass as well as for a higher heat transfer efficiency, provided that a pitched multiblade impeller at different heights is installed¹⁰.

Moreover, the internal heat transfer surface of the jacket is equal to about 21m², 15 of which are initially available on the basis of the initial filling degree of the reaction vessel.

During each reaction batch, 2200 kg of 4-Cl BTF (with average density and heat capacity equal to 1353kg/m³ and 1.257kJ/(kg °C), respectively³⁰) must be added in no more than three hours at the initial temperature of 60°C to 8350 kg of an anhydrous mixture of sulfuric and nitric acid containing

9-10% w/w of nitric acid (with average density and heat capacity equal to 1787kg/m³ and 1.477kJ/(kg °C), respectively), to produce 4-chloro, 3-nitro benzotrifluoride (in the following referred to as 4-Cl, 3-NO₂ BTF), according to the following reaction occurring in the continuous acidic phase^{10,12,26,27}:



In the current model, only the mono-nitration of 4-Cl BTF has been considered, becoming the second nitration rate relevant above 80°C^{26,27}: therefore, no selectivity issues have been taken into account.

As reported in the literature^{26,27}, the rate of reaction (10) can be described by the following equation:

$$r = 3.228 \cdot 10^{12} \cdot \exp\left(-\frac{87260}{8.314 \cdot T[\text{K}]}\right) \cdot m_A \cdot C_{A_d} \cdot C_{B_c} \quad (13)$$

where m_A is the average distribution coefficient of 4-Cl BTF, equal to 10⁻².

As can be noticed, in the rate equation (13) the contribution of the mixed acids dilution by the generated water (acting to lower the nitration rate) has been lumped for the sake of simplicity in the dependence on the nitric acid concentration, C_{B_c} . Such a simplification was possible since the nitric acid concentration is still high at each reaction extent, starting from an anhydrous system: in particular, even at the end of the reaction the equivalent water mass fraction in the sulfuric acid is as low as about 3%.

Under these conditions (stated by the chemical recipe) the system reactivity is relatively high¹⁰, so that for the expected industrial dosing times (of the order of hours), the accumulation of unreacted 4-Cl BTF is in any case limited below critical values.

The tests performed at the laboratory scale evidenced that the QFS operation of the reaction system requires an internal Westerterp number of about 30 with the heat transfer characteristics of the equipment used²⁷. Such a parameter is then kept constant during the process scale-up, according with the procedure described in the literature⁸.

However, the required Westerterp number can be reached at the industrial scale either through a relatively low heat transfer efficiency and a relatively high 4-Cl BTF dosing time, or through an enhanced heat transfer efficiency and a 4-Cl BTF dosing time fulfilling the required plant productivity.

As discussed in the following, since the reaction heat is relatively high (-123kJ/mol^{22,26,27}), in order to keep the 4-Cl BTF dosing time below the required three hours, the SBR must be equipped with an additional heat transfer surface^{26,27}.

However, the internal or external allocation of such an additional surface has a relevant influence on the SBR thermal behavior during the dosing period, and in particular on its variation in a narrow range above the recommended temperature (that is, 60°C).

In the following four heat transfer configurations are compared through the described sizing criterion and a final choice of the best option is suggested.

As a final consideration, it should be mentioned that especially for long dosing times and at relatively high temperatures, a partial decomposition of nitric acid can be observed¹⁰, which justifies the slight nitric acid excess typically adopted. Such a behavior leads to the production of NO_x gases leaving the system saturated with the generated water at the operating temperature and pressure, hence representing an additional heat removal contribution. This has not been considered in this case both for the sake of simplicity and because neglecting an additional heat removal term leads to a safer estimation of the external heat transfer surfaces.

A) SBR equipped with cooling jacket only

In this case, the SBR is equipped only with an internal heat transfer surface (given by the cooling jacket), which is initially available for about 15m².

With an overall heat transfer coefficient around 250 W/m²K for well agitated vessels^{11,16,17}, and according with the constraint:

$$Wt_{\text{int}} = \frac{(UA)_{0,\text{int}}t_{\text{dos}}}{\varepsilon(\rho C_P V)_0} = 30 \quad (14)$$

a 4-Cl BTF dosing time close to 9 hours should be adopted, that is, three times that required to match the plant productivity.

In Figure 6A the simulated reaction temperature profile is plotted: it can be noticed that even with a huge 4-Cl BTF dosing time, a more than 10°C temperature excursion above the initial value occurs. Moreover, the overall target temperature drop during the dosing period is higher than 3°C, that is well above the previously suggested range, corresponding to less than 1°C.

B) SBR equipped with cooling jacket and internal coil

Since the 4-Cl BTF dosing time calculated with the heat transfer configuration A) is three times than the desired value, in order to keep the same Westerterp number, a three times initial heat transfer surface must be adopted. Such a surface increase can be obtained through an about 40m² internal coil, 30 of which are available yet at the initial reactor filling degree. Therefore, the initial heat transfer surface is in this case around 45m² (that is, 15m² provided by the jacket and 30m² provided by the internal coil) and even with a 4-Cl BTF dosing time equal to 3 hours, the required Westerterp number can be kept.

It must be noticed that such an additional surface corresponds to an upper geometric limit reasonably achievable through an internal coil in the reaction vessel in question.

Moreover, since a 3 hours 4-Cl BTF dosing time matches at the limit the required plant productivity, the SBR behavior for coreactant dosing times even lower than 3 hours (in particular going from 2 to 3 hours) has been investigated.

In fact, starting from the required Westerterp number experimentally identified at the laboratory scale for the safe SBR operation, the scale-up procedure to the industrial reactor keeping the Westerterp number constant is conservative⁸, so that the reactor operation may be considered safe even at slightly lower dosing times.

In Figure 6B the simulated reactor temperature profiles for 4-Cl BTF dosing times equal to 2, 2.5 and 3h are plotted: it can be recognized that with respect to the heat transfer configuration A), the only relevant upgrade is the significant reduction of the coreactant dosing times (which in this case fulfill

the productivity requirements). However, the thermal reactor behavior in terms of peak reaction temperature during the supply period as well as of target temperature drop during the coreactant dosing are almost the same in the reaction run at $t_{\text{dos}}=3\text{h}$ (that is, at $Wt=30$ as in case A).

Moreover, as the 4-Cl BTF dosing time is reduced down to 2 hours, the target temperature variation during the supply period increases from 3 to 5°C, which is larger than 1°C.

C) External allocation of the internal coil heat transfer surface

The external allocation of the additional heat transfer surface (through an external heat exchanger installed on a reactor recycle loop), allows for easily overcoming the aforementioned constraints. According with the sizing criterion described in the previous sections, with this configuration the heat transfer surface can be limited only for keeping a measurable difference between the average reactor temperature and its initial value. In other cases, an upper limit to the external heat transfer surface arises from availability or installation issues of an oversized exchanger¹. However, such constraints are normally much weaker than those related to the installation of an internal coil within an existing reactor.

In this section the whole additional surface previously installed through an internal coil (equal to about 40m²) is supposed to be allocated externally through an equally sized heat exchanger to compare the effects of the external allocation of the same fraction of the whole heat transfer surface. Therefore, in this configuration, differently from case B), all the additional surface is fully available since the beginning of the supply period as summarized in Table 1.

It must be noticed that the external surfaces reported in Table 1 correspond to shell and tube exchangers: for different type of equipment (e.g., for plate or spiral exchangers), the values should be corrected through the ratio of the expected heat transfer coefficients in the two cases^{15,16,17,21}, keeping the UA product constant.

On the basis of the estimated overall heat transfer coefficients for the reactor jacket^{11,17} (that is, 250 W/m²K) and for an external shell and tube exchanger^{16,17,21} (that is, 230W/m²K), the internal and external Westerterp numbers for $t_{\text{dos}}=3\text{h}$ are equal respectively to:

$$Wt_{\text{int}} = \frac{(UA)_{\text{0,int}}t_{\text{dos}}}{\varepsilon(\rho C_P V)_0} \approx 10 \quad (15)$$

$$Wt_{\text{ext}} = \frac{(UA)_{\text{0,ext}}t_{\text{dos}}}{\varepsilon(\rho C_P V)_0} \approx 24 \quad (16)$$

It can be noticed that for $t_{\text{dos}}=3\text{h}$ the overall Westerterp number (equal to 34) is in this case slightly higher than in case B) even with the same overall heat transfer efficiency: this because a relevant fraction of such a surface is here fully available since from the beginning of the supply period.

In Figure 6C the simulated reactor temperature profiles for 4-Cl BTF dosing times equal to 2, 2.5 and 3 hours are plotted: it can be recognized that with respect to the heat transfer configuration B), the only relevant upgrade is the reduction of the target temperature drops during the supply period down to 30% of the former values. In particular decreasing the coreactant dosing time from 3 to 2 hours, the target temperature variation during the supply period increases from 1 to 1.5°C, instead of from 3 to 5°C with the configuration B). Therefore, as expected on the basis of Equation (7), the external allocation of a fraction of the overall heat transfer surface has an impact on the mitigation of the reactor temperature variation during the supply period. However, the target temperature variation, ΔT_{ta} , is still slightly above 1°C. Therefore, neither in this case the target temperature should be taken as a reference value in order to check the system reactivity during the 4-Cl BTF supply.

Moreover, even for $t_{\text{dos}}=3\text{h}$ the peak reaction temperature is still around 70°C, that is, only slightly lower than that for case B): this is also logical since from case B) to C) the overall heat transfer surface is the same, even if with a different extent of its initial availability.

Also the difference between the average target temperature and the initial temperature is still close to 10°C for $t_{\text{dos}}=3\text{h}$ and hence higher than the lower limit for monitoring the reaction under QFS conditions.

D) SBR equipped with cooling jacket and a properly sized external exchanger

In this case, the external heat exchanger is sized with the only constraints of a measurable difference between the average and initial reaction temperatures during the 4-Cl BTF supply and of a not oversized heat transfer surface, because of economical and/or installation issues¹. In particular, with reference to a shell and tube heat exchanger (with its typical range of design heat transfer coefficients^{16,17,21}), an upper limit of the external surface equal to 150m² is fixed for the considered reactor.

With $R_{\Delta T}=0.2$, from the graphical correlation of Figure 3, a required external Westerterp number:

$$Wt_{\text{ext}} = \frac{(UA)_{\text{ext}} t_{\text{dos}}}{\varepsilon(\rho C_P V)_0} = 61.5 \quad (17)$$

can be estimated.

On the basis of an expected overall heat transfer coefficient equal to 230W/(m²K) for properly operated shell and tube exchangers^{16,17,21}, a required external surface equal to about 106m² can be calculated, which is finally approximated to the upper standard size of 120m², in compliance with the stated upper limit of 150m² and corresponding to an external Westerterp number equal to 70.

However, a plate equipment is in this case preferable since it provides five times higher heat transfer coefficients (of the order of 1000W/m²K¹⁵) and hence a roughly five times lower heat transfer surface, as well as a lower circulation rate of the reaction mass through it.

From the adiabatic temperature rise referred to the initial reactor load:

$$\Delta T_{\text{ad},0} = \frac{(-\Delta \tilde{H}_r) \times n_{4\text{-Cl BTF},1}}{(m \tilde{C}_P)_0} \approx 122^\circ\text{C} \quad (18)$$

and from the selected $R_{\Delta T}$ value (equal to 0.2), an expected target temperature variation of about 0.2°C can be estimated for a 4-Cl BTF dosing time equal to 3 hours.

In Figure 6D the temperature time profiles of the SBR for $t_{\text{dos}}=2, 2.5$ and 3h are plotted: it can be noticed that the variation of the target temperature during the supply period, ΔT_{ta} , increases from 0.2 to 0.3°C as the coreactant dosing time decreases from 3 down to 2 hours, which is always lower than 1°C.

Moreover, in this case the significant increase of the overall heat transfer efficiency (expressed by an overall Westerterp number of 80 vs. 30) with respect to the previous configurations allows for keeping the reaction temperature only 4°C in average above the initial value for $t_{\text{dos}}=3\text{h}$ and almost constant for the most part of the supply period. Such a temperature difference is at the same time higher than the minimum ΔT_{meas} value of 2°C for detecting the expected reaction triggering during the supply period.

As a final check, with a 4°C difference between the reactor and the coolant temperatures, the average heat removal rate through the jacket for $t_{\text{dos}}=3\text{h}$ is equal to:

$$\dot{Q}_{\text{internal}} \sim 250 \text{ W/m}^2\text{K} \times 18 \text{ m}^2 \times 4^\circ\text{C} / 1000 = 18\text{kW} \quad (19)$$

where 18m² is the average heat transfer surface between the beginning and the end of the supply period.

The heat removal rate through the external heat exchanger is instead equal to:

$$\dot{Q}_{\text{external}} \sim 1000 \text{ W/m}^2\text{K} \times 30 \text{ m}^2 \times 4^\circ\text{C} / 1000 = 120 \text{ kW} \quad (20)$$

The sum of these two duties (equal to about 138 kW) roughly matches the enthalpy contribution of the reaction, which, under QFS conditions is equal to the product of the 4-Cl BTF feed rate times the reaction heat:

$$\dot{Q}_{\text{reaction}} = 2200 \text{ kg}/180.5 \text{ kg/kmol} \times \frac{1}{10800 \text{ s}} \times 123000 \text{ kJ/kmol} = 139\text{kW} \quad (21)$$

The selected exchanger size allows therefore for both minimizing the target temperature variation during the supply period and measuring the difference between current and initial temperatures, monitoring in this way the SBR operation under QFS conditions.

Performing the reaction under such controlled conditions has then a positive effect on the amount of impurities as well as on the color of the final product, which is normally negatively affected by excessive temperature peaks during the 4-Cl BTF supply^{10,12,13}.

As a final consideration it is worth noticing that in all the considered options, a uniform 4-Cl BTF dosing rate has been adopted. Instead, at the industrial scale a two steps dosing strategy could be even

adopted: an initial fraction of the supply period in which the system reactivity is higher and the SBR is operated at a lower 4-Cl BTF dosing rate followed by a final part where the feed could be significantly accelerated, due to the lower system reactivity to be expected when nitric acid is progressively consumed. Adopting such a dosing strategy could lead to a lower heat transfer surface requirement, since the heat evolution is lowered where the system reactivity is potentially higher: even if this option has not been taken into account in the development of the presented sizing procedure of the external heat transfer surface, it could be a useful operating strategy whenever a single multipurpose SBR had to be used for different reaction processes, some of which would require a higher heat transfer surface because of their exothermic behavior.

It must be finally taken into account that the described sizing procedure of the external heat transfer surface for isoperibolic SBRs is in general affected by estimation errors of the involved process parameters. In particular, among the variables required for the calculation of $W_{t_{ext}}$ through Equation (9), estimation errors of the reaction heat (and hence of the adiabatic temperature rise, $\Delta T_{ad,0}$) and/or of the internal heat transfer coefficient (and hence of the internal Westerterp number, $W_{t_{int}}$) can be reasonably expected at the industrial scale: of the remaining parameters, in fact, R_H has a negligible influence on the calculated $W_{t_{ext}}$ and ε is a well-defined recipe parameter.

It should be noted that whereas the reaction heat is usually accurately estimated through e.g. calorimetric tests²², the overall heat transfer coefficients are much more affected by estimation errors, due e.g. to unforeseen fouling phenomena^{16,17,21}.

$\Delta T_{ad,0}$ affects the estimated target temperature variation across the dosing period, ΔT_{ta} , at the selected $R_{\Delta T}$ value: in the current industrial case (for which ΔT_{ta} is equal to 0.25°C as a consequence of an assumed $R_{\Delta T}$ of 0.2 and a $\Delta T_{ad,0}$ of 122°C), even a $\pm 25\%$ error on the adiabatic temperature rise (that is from 90 to 150°C), would lead to a ΔT_{ta} value ranging from 0.2 to 0.3°C; such a variation is not relevant from a practical point of view. However, a $\pm 25\%$ error on the $W_{t_{int}}$ (typically related to an error in the estimation of the internal overall heat transfer coefficient) leads to a $W_{t_{ext}}$ ranging from

55 to 65 vs. the calculated value of 61.5: therefore, the $W_{t_{ext}}$ variation is only $\pm 10\%$ (with respect to a $\pm 25\%$ error on $W_{t_{int}}$) and falls within the normally assumed safety factor when sizing a heat exchanger.

5. Conclusions

A number of potential runaway reactions of the fine chemical and pharmaceutical industry need to be performed in isoperibolic SBRs with enhanced heat transfer surface in order to speed up the coreactant supply, hence reducing the cycle time per batch. The external allocation of the enhancing heat transfer surface mitigates the temperature variations under the QFS regime, allowing for a better control of the reaction conditions and for monitoring the system reactivity level through the reactor temperature value. In this work, a kinetic-free criterion has been developed for isoperibolic SBRs through which the external heat exchange surface area required to make the reactor operation quasi-isothermal can be estimated.

Nomenclature

A	component A (dosed coreactant)
A	heat transfer surface, m ²
B	component B (reactant initially loaded in the reactor)
C	component C (reaction product)
C _i	molar concentration, kmol/m ³
\tilde{C}_P	molar heat capacity at constant pressure, kJ/(kmol·K)
\hat{C}_P	mass heat capacity at constant pressure, kJ/(kg·K)
d	dispersed phase nominal diameter, m
D	component D (reaction product)
D _L	diffusion coefficient in the liquid phase, m ² /s
Da	= $k_R \cdot t_{dos} \cdot C_{B0}^{n+m-1}$, Damköhler number, -
E	activation energy, kJ/kmol
f	function of ϑ and ζ in Eq. 2
k	kinetic constant, m ³ /(kmol·s)
m	mass, kg
m	order of reaction with respect to reactant B, -
m _A	= C _{A,c} /C _{A,d} , distribution coefficient of A, -
m _B	= C _{B,d} /C _{B,c} , distribution coefficient of B, -
n	number of moles, kmol
n	order of reaction with respect to reactant A, -
\dot{Q}	heat duty, kW
r	reaction rate, kmol/(m ³ ·s)
R	=8.314kJ/kmol K, ideal gas constant
R _{ΔT}	= $\frac{\Delta T_{ta}}{\Delta T_{ad,0}} \times 100$, ΔT ratio, -
R _H	= $(\rho C_P)_{dos}/(\rho C_P)_0$, heat capacity ratio, -
RE	reactivity enhancement factor, -
t	time, s (or h, where specified)
T	temperature, K
ΔT _{ad,0}	= $\frac{(-\Delta \tilde{H}_r) \times n_{A1}}{(\hat{\rho} \tilde{C}_P V)_c}$, adiabatic temperature rise, K
ΔT _{ta}	= T _{ta,0} - T _{ta,1} , overall target temperature variation during the supply period, K
U	overall heat transfer coefficient, kW/(m ² K)
V	volume, m ³
Wt	= $\frac{(UA)_0 \cdot t_{dos}}{\varepsilon \cdot (\hat{\rho} \cdot \tilde{C}_P \cdot V_r)_0}$, Westerterp number, -

Subscripts and superscripts

4-Cl BTF	4-chloro benzotrifluoride
ad	adiabatic
app	apparent
A	component A (dosed coreactant)
B	component B (reactant initially loaded in the reactor)
b	bubble or drop
band	band of variation
C	component C (reaction product)
c	continuous phase

cool	coolant or cooling
d	dispersed phase
D	component D (reaction product)
dos	dosing
eff	effective
ext	external
ε	error
int	internal
m	order of reaction with respect to reactant B, -
max	maximum
meas	measured
n	order of reaction with respect to reactant A, -
r	reaction
R	reference
ta	target
0	start of the semibatch period
1	end of the semibatch period or internal band of temperature variation
2	external band of temperature variation

Greek symbols

α	flag parameter in Eqs. 4 and 6
γ	$=E/(RT_R)$, dimensionless activation energy, -
$\Delta\tilde{H}$	reaction enthalpy, kJ/kmol
ΔT	temperature rise or difference, K
$\Delta\tau$	dimensionless temperature rise or difference, -
ε	$=V_{dos,1}/V_{r0}$, relative volume increase, -
ζ	conversion of B, -
ϑ	$=t/t_{dos}$, dimensionless time, -
ν	stoichiometric coefficient, -
$\tilde{\rho}$	molar density, kmol/m ³
$\hat{\rho}$	mass density, kg/m ³
τ	dimensionless temperature, -
Φ	function
X	X number, -
Ψ	Ψ number, -

References

- (1) Douglas, J. M. *Conceptual Design of Chemical Processes*; McGraw Hill: New York, 1988.
- (2) Steinbach, J. *Safety Assessment for Chemical Processes*; Wiley-VCH: Weinheim, 1999.
- (3) Zaldívar, J.M.; Cano, J.; Alós, M.A.; Sempere, J.; Nomen, R.; Lister, D.; Maschio, G.; Obertopp, T.; Gilles, E.D.; Bosch, J.; Strozzi, F. A General Criterion to define Runaway Limits in Chemical Reactors. *J. Loss Prevent. Proc.* **2003**, *16* (3), 187.
- (4) Steensma, M.; Westerterp, K. R. Thermally Safe Operation of a Cooled Semibatch Reactor. Slow Liquid-Liquid Reactions. *Chem. Eng. Sci.* **1988**, *43*, 2125.
- (5) Steensma, M.; Westerterp, K. R. Thermally Safe Operation of a Semibatch Reactor for Liquid-Liquid Reactions. Slow Reactions. *Ind. Eng. Chem. Res.* **1990**, *29*, 1259.
- (6) Steensma, M.; Westerterp, K. R. Thermally Safe Operation of a Semibatch Reactor for Liquid-Liquid Reactions. Fast Reactions. *Chem. Eng. Technol.* **1991**, *14*, 367.
- (7) Maestri, F.; Rota, R. Safe and Productive Operation of Homogeneous Semibatch Reactors. I: Development of a General Procedure. *Ind. Eng. Chem. Res.* **2006**, *45*, 8002.
- (8) Maestri, F.; Copelli, S.; Rota, R.; Lunghi, A.; Gigante, L.; Cardillo, P. Simple Procedure for Optimal Scale-up of Fine Chemical Processes. I: Practical Tools. *Ind. Eng. Chem. Res.* **2009**, *48*, 1307.
- (9) Casson Moreno, V.; Lister, D.G.; Milazzo, M.F.; Maschio, G. Comparison of Criteria for Prediction of Runaway Reactions in the Sulphuric Acid Catalyzed Esterification of Acetic Anhydride and Methanol. *J. Loss Prevent. Proc.* **2012**, *25*(1), 209.
- (10) Albright, L. F. Nitration. In *Kirk Othmer – Encyclopedia of Chemical Technology*; Third Ed.; Wiley & Sons: New York, 1981; Vol. 15, p. 841.
- (11) Westerterp, K. R.; Molga, E. J. No More Runaways in Fine Chemical Reactors. *Ind. Eng. Chem. Res.* **2004**, *43*, 4585.
- (12) Morrison, R. T.; Boyd, R. N. *Organic Chemistry*; Sixth Ed., Prentice Hall of India, New Delhi, 2002.

- (13) Smith, M.; March, J. *Advanced Organic Chemistry: Reactions, Mechanisms and Structure*; Sixth Ed., Wiley, New York, 2007.
- (14) Stephanopoulos, G. *Chemical Process Control: An Introduction to Theory and Practice*; First Ed., Prentice-Hall, Englewood Cliffs - New Jersey, 1984.
- (15) Alfa Laval, *Thermal Handbook*, 1989.
- (16) Branan, C. R. *Rules of Thumb for Chemical Engineers*; Fourth Ed., Gulf Professional Publishing, Burlington, 2005.
- (17) Kern, D.Q. *Process Heat Transfer*; International Student Ed., Mc Graw Hill, New York, 1983.
- (18) Maestri, F.; Rota, R. Kinetic-Free Safe Operation of Fine Chemical Runaway Reactions: a General Criterion. *Ind. Eng. Chem. Res.* **2016**, *55*, 925.
- (19) Maestri, F.; Rota, R. Simple Monitoring of Semibatch Polymerization Processes: An Integrated Criterion. *Ind. Eng. Chem. Res.* **2017**, *56*, 7434.
- (20) Maestri, F.; Copelli, S.; Rizzini, M.; Rota, R. Safe and Selective Monitoring of Consecutive Side Reactions. *Ind. Eng. Chem. Res.* **2017**, *56*, 11075.
- (21) Perry, R. H.; Green, D. W. *Chemical engineers' handbook*; Eight Edition, McGraw Hill, 2008.
- (22) Cardillo, P. *Incidenti in Ambiente Chimico. Guida allo Studio e alla Valutazione delle Reazioni Fuggitive*; Stazione Sperimentale per i Combustibili: San Donato Milanese, 1998 (*in Italian*).
- (23) Casson Moreno, V.; Maschio, G. Screening Analysis for Hazard Assessment of Peroxides Decomposition. *Ind. Eng. Chem. Res.* **2012**, *51*(22), 7526.
- (24) Vianello, C.; Salzano, E.; Broccanello, A.; Manzardo, A.; Maschio, G. Runaway Reaction for the Esterification of Acetic Anhydride with Methanol Catalyzed by Sulfuric Acid. *Ind. Eng. Chem. Res.* **2018**, *57*(12), 4195.
- (25) Copelli, S.; Derudi, M.; Cattaneo, C. S.; Nano, G., Raboni, M.; Torretta, V.; Rota, R. Synthesis of 4-Chloro-3-nitrobenzotrifluoride: Industrial Thermal Runaway Simulation due to Cooling System Failure. *Process. Saf. Environ.* **2014**, *92*, 659.

- (26) Maestri, F.; Copelli, S.; Rota, R.; Lunghi, A.; Gigante, L.; Cardillo, P. Simple Procedure for Optimal Scale-up of Fine Chemical Processes. II: Nitration of 4-Chlorobenzotrifluoride. *Ind. Eng. Chem. Res.* **2009**, *48* (3), 1316.
- (27) Maestri, F.; Rota, R. Kinetic-Free Safe Optimization of a Semibatch Runaway Reaction: Nitration of 4-Chloro Benzotrifluoride. *Ind. Eng. Chem. Res.* **2016**, *55*, 12786.
- (28) Copelli, S.; Derudi, M.; Maestri, F.; Rota, R. Safe operating conditions for semibatch processes involving consecutive reactions with autocatalytic behavior. *Chem. Eng. Sci.* **2010**, *65*, 5464.
- (29) Westerterp, K. R.; van Swaaij, W. P. M.; Beenackers, A. A. C. M. *Chemical Reactor Design and Operation*; Wiley, Chichester, 1984.
- (30) Yaws, C. L. *Chemical Properties Handbook*; McGraw Hill, 1998.

Tables

Case	Heat transfer Surface	Initial	Final
A)	Jacket	15m ²	21m ²
	Internal coil	-	-
	External shell and tube exchanger	-	-
	TOTAL A)	15m²	21m²
B)	Jacket	15m ²	21m ²
	Internal coil	30m ²	40m ²
	External shell and tube exchanger	-	-
	TOTAL B)	45m²	61m²
C)	Jacket	15m ²	21m ²
	Internal coil	-	-
	External shell and tube exchanger	40m ²	40m ²
	TOTAL C)	55m²	61m²
D)	Jacket	15m ²	20m ²
	Internal coil	-	-
	External shell and tube exchanger	120m ²	120m ²
	TOTAL D)	135m²	140m²

Table 1. Mixed acids nitration of 4-Cl BTF in a 9m³ SBR: heat transfer surface contributions at the beginning and at the end of the supply period for different heat transfer setups.

Captions to the figures

Figure 1. Process flow diagram of an isoperibolic SBR equipped with an external heat exchanger on the reactor recycle line.

Figure 2. Isoperibolic SBR for homogenous reaction systems ($R_H=1$). Estimated $W_{t_{ext}}$ values vs. $W_{t_{int}}$ for different ε values and $R_{\Delta T}=0.05$ (A); 0.1 (B); 0.2 (C); 0.5 (D) and 1 (E).

Figure 3. Isoperibolic SBR for heterogeneous liquid-liquid reaction systems with an aqueous continuous phase ($R_H=0.4$). Estimated $W_{t_{ext}}$ values vs. $W_{t_{int}}$ for different ε values and $R_{\Delta T}=0.05$ (A); 0.1 (B); 0.2 (C); 0.5 (D) and 1 (E).

Figure 4. Isoperibolic SBR for heterogeneous liquid-liquid reaction systems with an organic continuous phase ($R_H=2.5$). Estimated $W_{t_{ext}}$ values vs. $W_{t_{int}}$ for different ε values and $R_{\Delta T}=0.05$ (A); 0.1 (B); 0.2 (C); 0.5 (D) and 1 (E).

Figure 5. Flow chart summarizing the presented sizing criterion of the external heat transfer surface for isoperibolic SBRs.

Figure 6. Isoperibolic 9m^3 SBR for the mixed acid nitration of 4-Cl BTF. $T_{cool}=T_0=60^\circ\text{C}$. Mixed acids initial composition: $\sim 9\%$ w/w of nitric acid. $t_{dos}=9\text{h}$ for case (A) and 2, 2.5 and 3h for cases (B), (C) and (D). Temperature-time profile for: cooling jacket only (A); cooling jacket plus a 40m^2 internal coil (B); cooling jacket plus a 40m^2 external shell and tube exchanger (C); cooling jacket plus a 120m^2 external shell and tube exchanger (D).

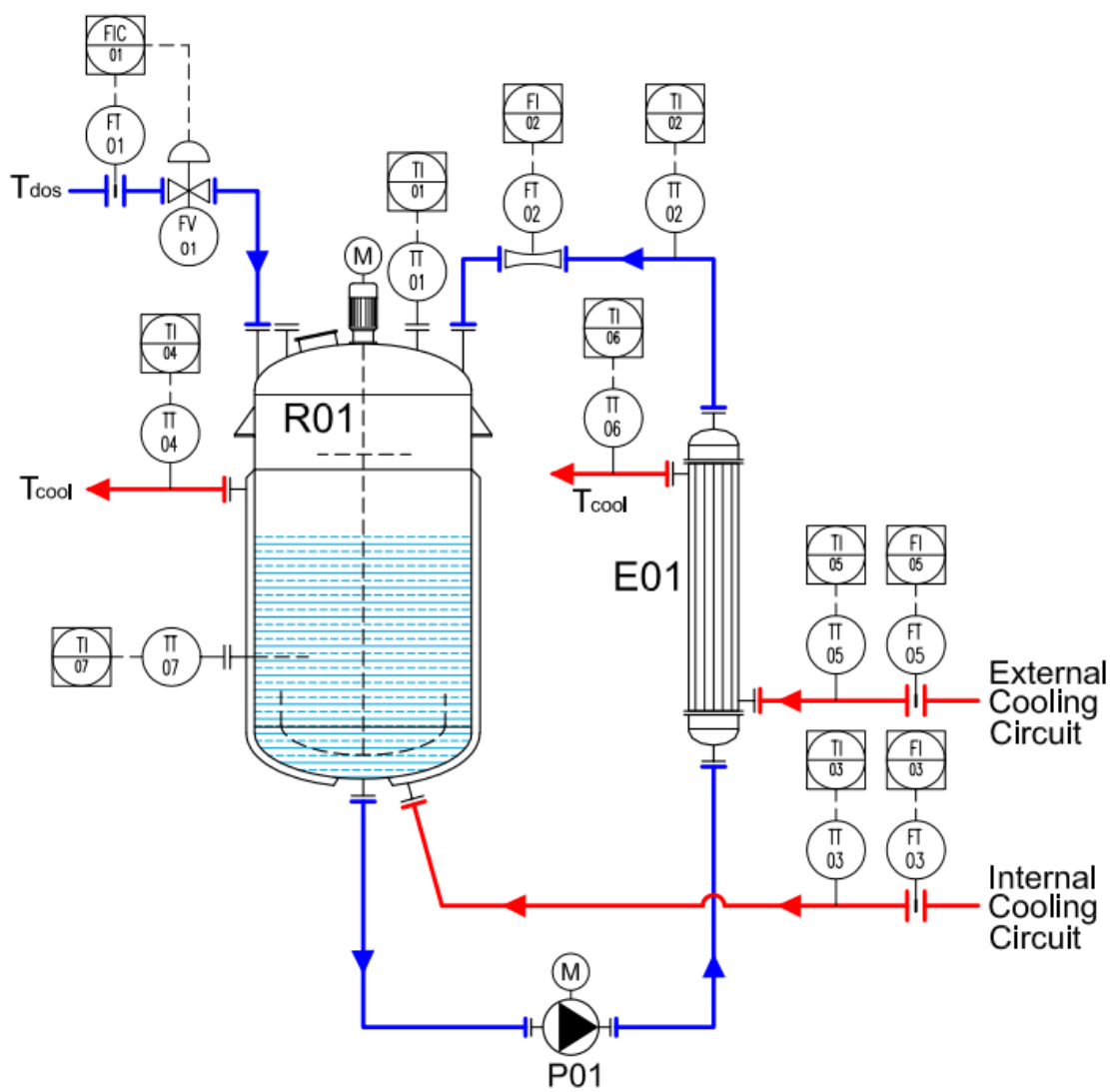


Fig. 1

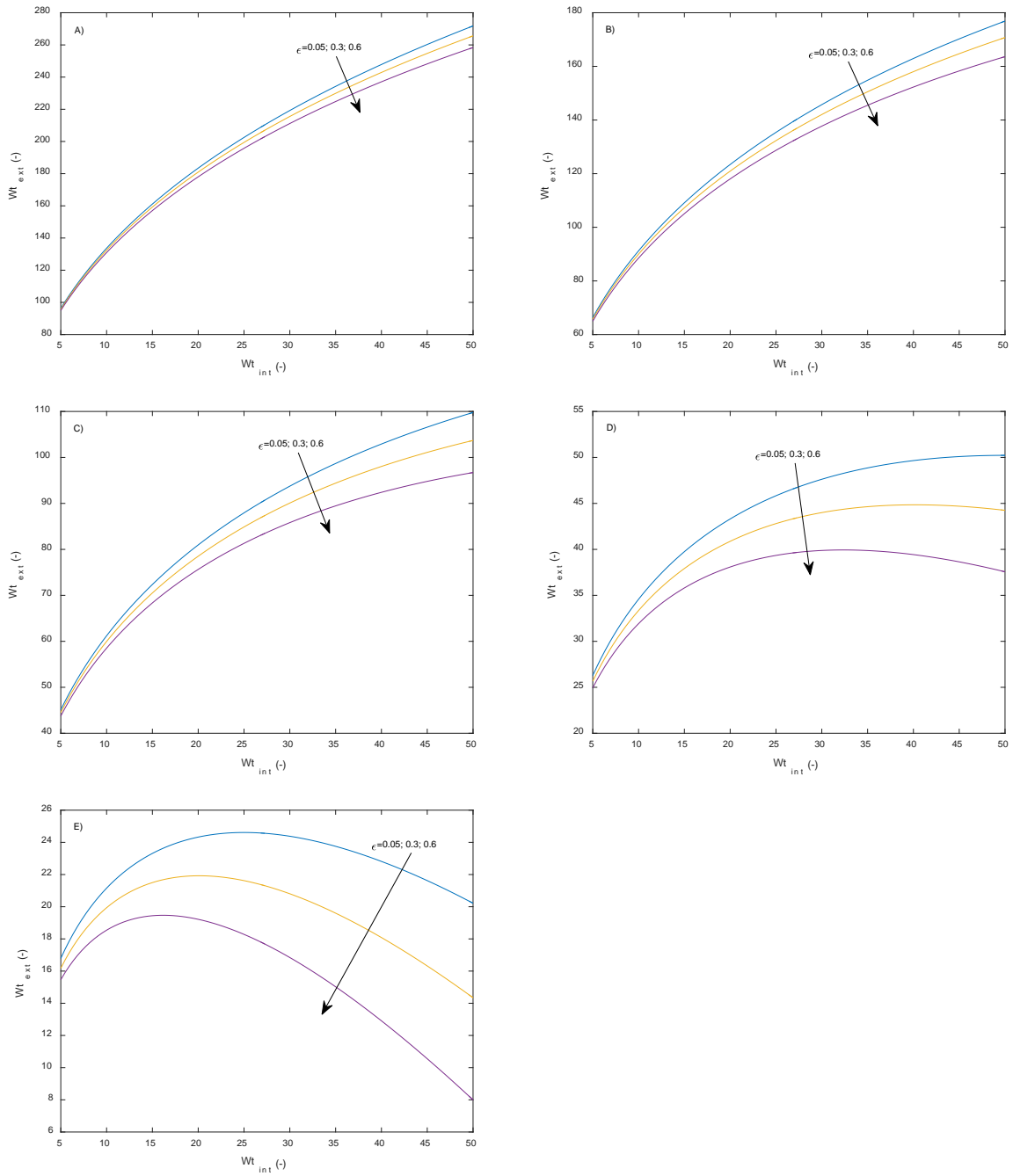


Fig. 2

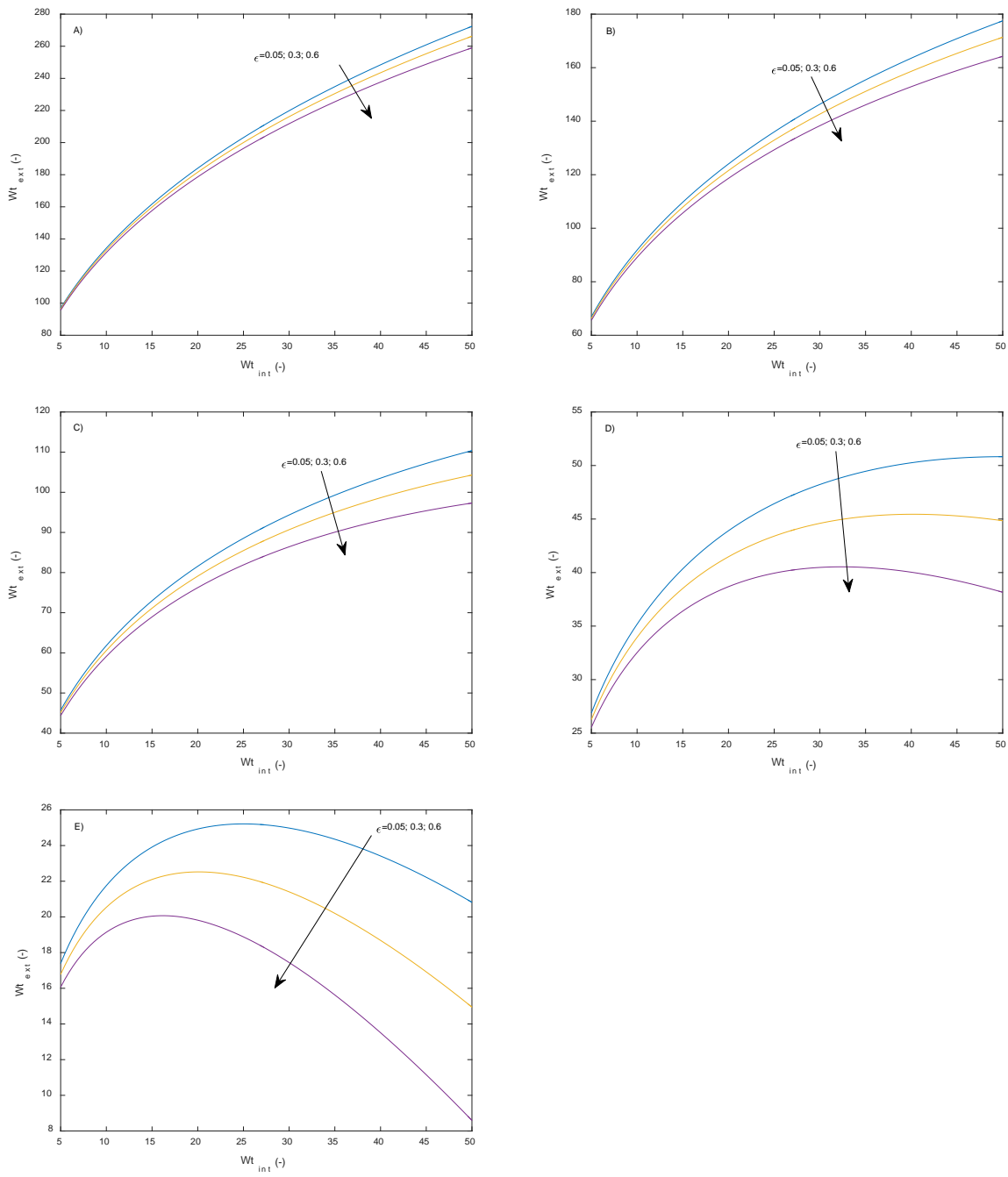


Fig. 3

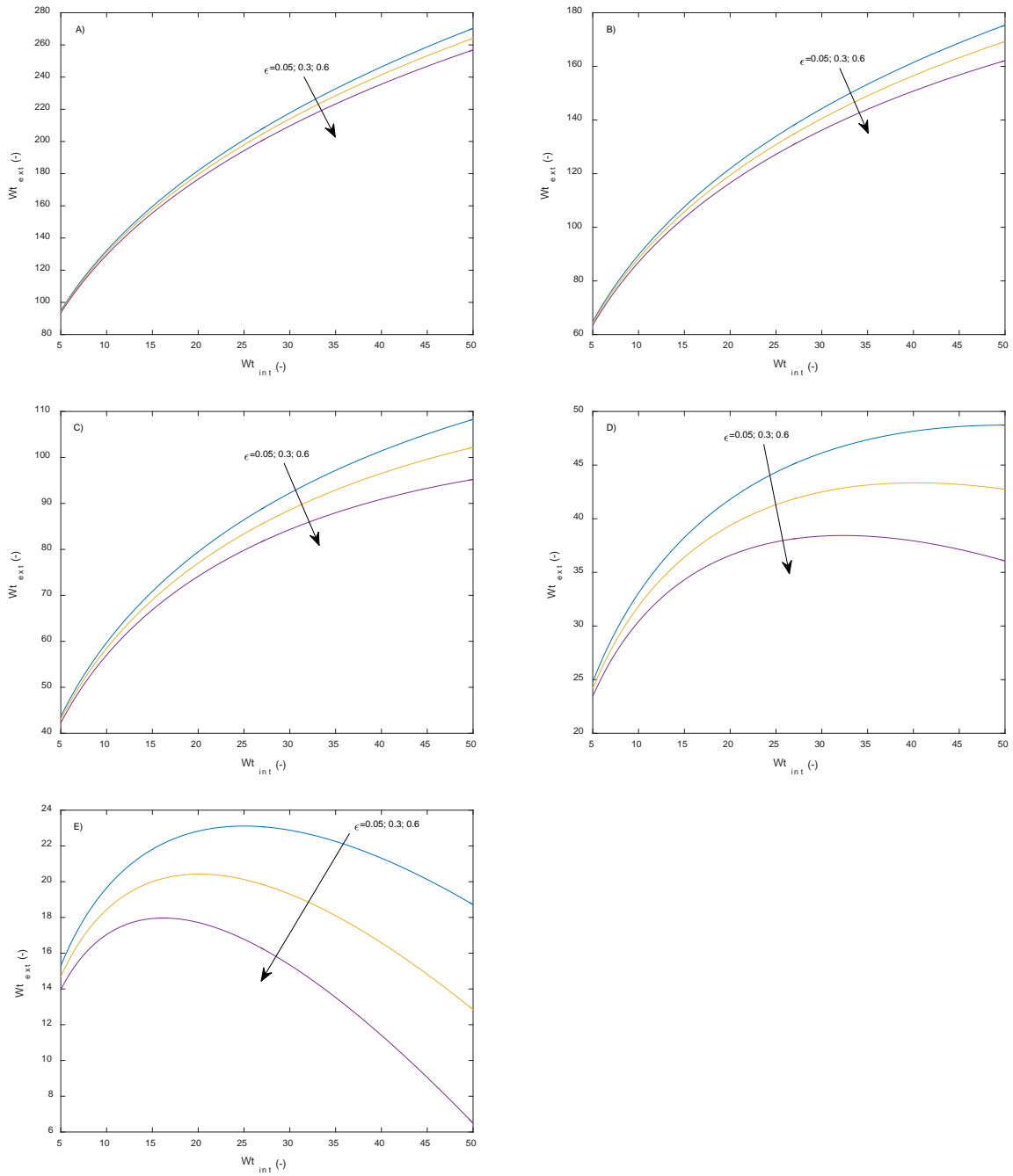


Fig. 4

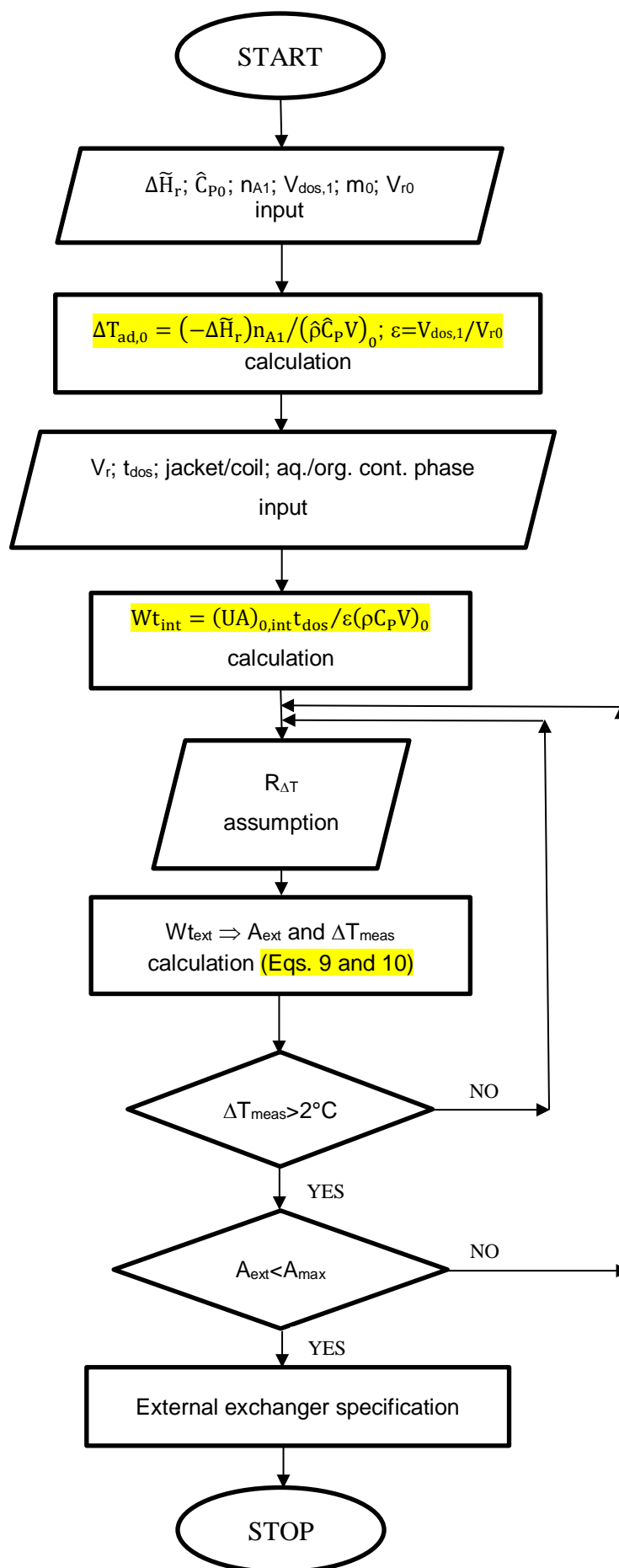


Fig. 5

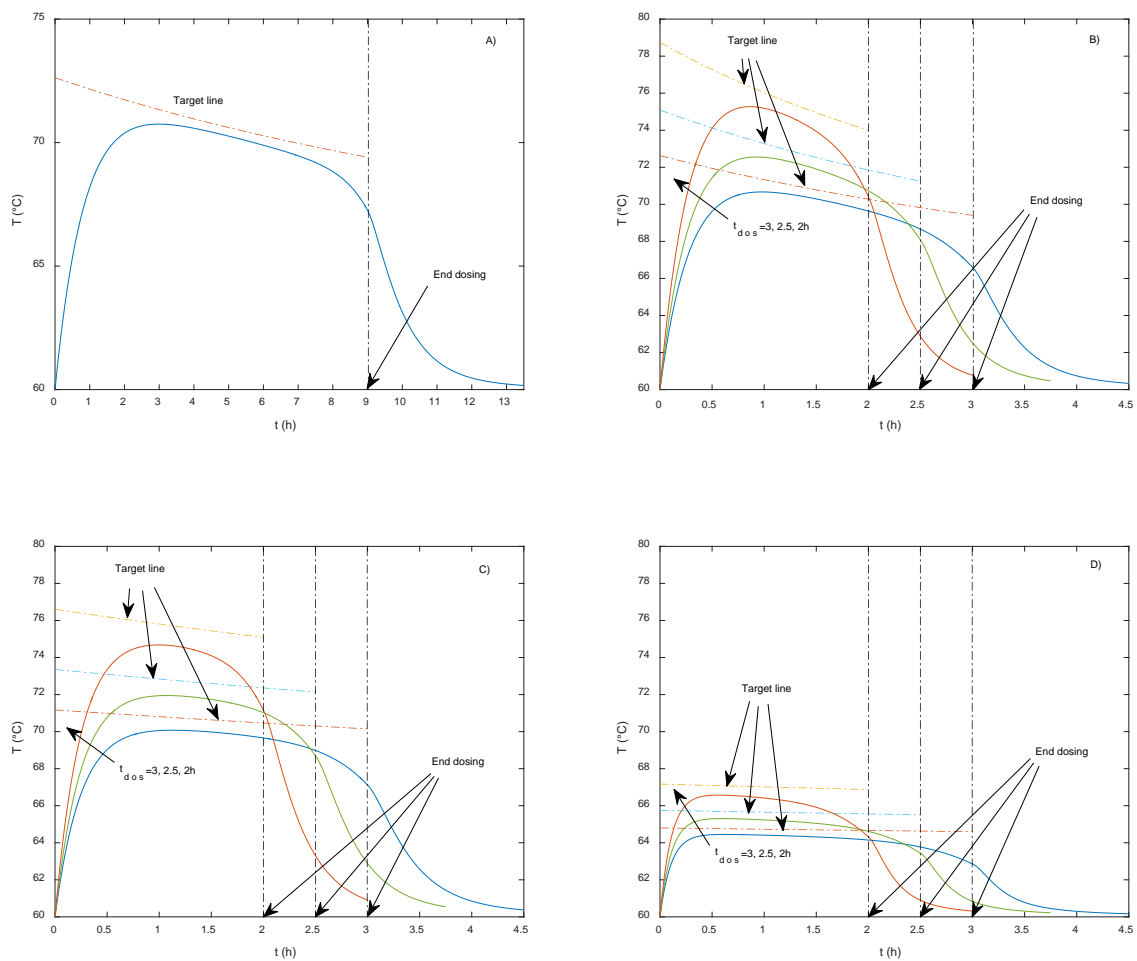


Fig. 6

For Table of Contents Only

